

# Trapping and observing single atoms in the dark

T. Puppe, I. Schuster, A. Grothe, A. Kubanek, K. Murr, P.W.H. Pinkse, and G. Rempe\*  
*Max-Planck-Institut für Quantenoptik, Hans-Kopfermann-Str. 1, D-85748 Garching, Germany*  
(Dated: February 1, 2008)

A single atom strongly coupled to a cavity mode is stored by three-dimensional confinement in blue-detuned cavity modes of different longitudinal and transverse order. The vanishing light intensity at the trap center reduces the light shift of all atomic energy levels. This is exploited to detect a single atom by means of a dispersive measurement with 95 % confidence in  $10 \mu\text{s}$ , limited by the photon-detection efficiency. As the atom switches resonant cavity transmission into cavity reflection, the atom can be detected while scattering about one photon.

PACS numbers: 32.80.-t, 32.80.Pj, 42.50.-p

A single atom coupled to a single mode of a high-finesse optical cavity constitutes an ideal system for the investigation of matter-light interaction at the level of individual quanta. Any application of this system, e.g. in quantum information science [1], relies on the ability to precisely localize the atom within the cavity mode at regions of strong atom-cavity coupling. An established tool to reach this goal is an optical dipole-force trap [2]. So far, only traps with lasers red detuned from the atom have been demonstrated in cavity quantum electrodynamics (QED) [3, 4, 5, 6]. In such a red-detuned dipole trap, the atom is attracted towards intensity maxima. While this has the advantage that a single light mode is sufficient, it has the disadvantage that the high laser intensity perturbs the atom. As a consequence, the dynamic Stark effect shifts the atomic energy levels and, hence, the transition frequency. Moreover, increasing the trap depth for better localization of the atom will increase the Stark shift. For some atoms, like cesium, the Stark shift of a particular transition *between* certain energy levels vanishes in a red dipole trap at a magic wavelength [7]. An alternative approach is to use a blue-detuned light field for trapping. Here the atom is repelled from the high-intensity region and, hence, trapped close to an intensity minimum. Such a trap has the advantage that the Stark shift of *all* states can be very small so that the free-space properties of the atom are largely retained. Superposition states, for example, will be less affected by the trapping potential.

In this Letter we report on trapping single rubidium atoms in a blue-detuned intracavity dipole trap. We show that the Stark shift of the atomic transition vanishes while the atom is strongly coupled to a cavity mode. The blue trap allows us to explore the regime of dispersive single-atom observation. As a proof of principle, we demonstrate that the atom is efficiently detected while scattering only a few spontaneous photons.

The idea of the blue trap is to use far-detuned cavity modes to shape a potential landscape which realizes three-dimensional confinement around a dark trap center (Fig. 1). The standing wave of the high-finesse cavity guarantees maximum contrast of the interference

pattern. The trap center is therefore accurately dark. Such a blue trap has a number of advantages for experiments in cavity QED: (1) Since the trap height does not contribute to the atomic detuning, it can be made large for good confinement. (2) An atom inside the trap is well isolated by the surrounding potential barrier, outside atoms are repelled. (3) The blue trap can be loaded by creating a dark funnel to guide a slow atom to the trap center. As the atom is repelled from the blue light, the kinetic energy does not increase during the capture process. Moreover, weakly coupled atoms that are not collected by the funnel are rejected. (4) The funnel can be closed upon detection of the strongly coupled atom in the trap center. Because the energy gain due to guiding and switching is kept small, the requirement to cool

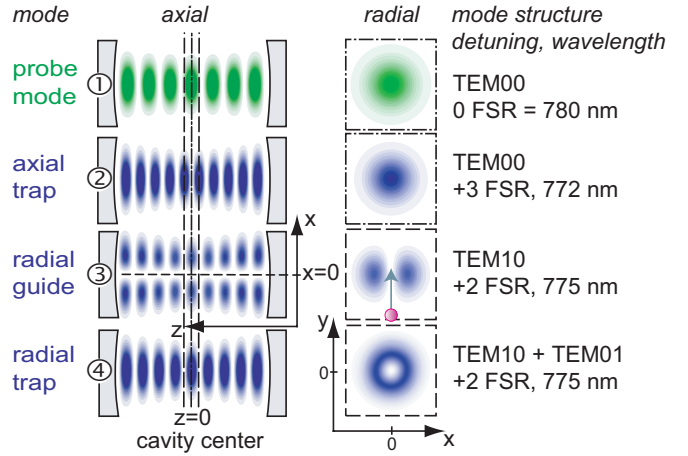


FIG. 1: (Color online) The blue intracavity dipole trap from the perspective of an entering atom. The slow atom is restricted to the field minima of the blue light fields that coincide with the antinodes of the near-resonant probe mode ① at the cavity center. Persistent *axial* confinement is provided by a  $\text{TEM}_{00}$  mode ②, “pancakes”. Combined with the *transverse* nodal line of a  $\text{TEM}_{10}$  mode ③, “funnels” are formed to guide the atom to a strong-coupling region. Full three-dimensional confinement is achieved by adding a  $\text{TEM}_{01}$  mode to complete a transverse “doughnut” mode ④.

the atom after the capture process is relaxed. (5) Since during the whole loading sequence the atomic detuning is preserved, parameter regimes of large cavity-enhanced heating [8, 9] can be avoided.

The experimental setup presented in Fig. 2 is an extension of the one described in detail elsewhere [10, 11]. The intracavity dipole potential is created by a combination of standing-wave cavity modes of different longitudinal and transverse mode order (Fig. 1), all blue detuned with respect to the near-resonant cavity QED probe field: persistent axial confinement along the cavity axis is provided by a TEM<sub>00</sub> mode ② detuned by an odd number of free-spectral ranges (FSR). The oblate antinodes (“pancakes”) of this mode confine the atom to the nodal planes that overlap with the antinodes of the probe mode ① halfway between the mirrors. Radial confinement is provided by a doughnut mode ④ formed by a combination of TEM<sub>10</sub> and TEM<sub>01</sub> modes detuned by an even number of FSR. To load an atom into the trap, the radial confinement is relaxed by using the TEM<sub>10</sub> mode only. Slow atoms from an atomic fountain are injected from below along the  $y$ -direction. They are guided towards the cavity center at  $x = 0$  along the nodal line of this TEM<sub>10</sub> mode ③. The combination of axial confinement and transverse guiding creates funnels that direct the atom to the antinodes of the probe mode ①. Note that the axial confinement need not be switched to close the trap. Since the axial and radial characteristics of the trap are defined by independent modes at different frequencies they can be controlled individually.

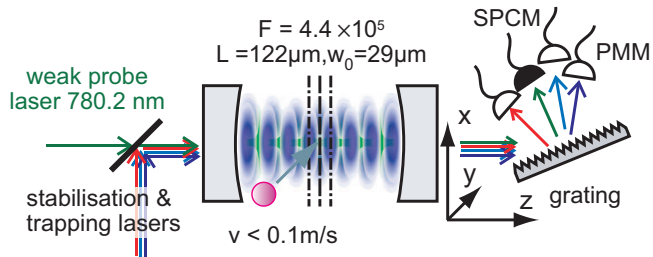


FIG. 2: (Color online) Experimental setup. Slow  $^{85}\text{Rb}$  atoms are injected from below into a high-finesse cavity. The cavity is excited by a weak near-resonant probe field at 780.2 nm and strong blue-detuned dipole fields. Behind the cavity, a grating directs the probe light onto single-photon counting modules (SPCM) whereas all dipole beams are detected by photomultiplier modules (PMM). The cavity length  $L = 0.122\text{ mm}$  is independently stabilized by a weak laser at 785.2 nm. Midway between the mirrors, the trap center coincides with an antinode of the probe field. The mode profiles in the dash-dotted and the dashed central plane are discussed in Fig. 1. The waist of the 780.2 nm fundamental transverse mode is  $w_0 = 29\text{ }\mu\text{m}$ , and  $F = 4.4 \times 10^5$  is the cavity finesse. The maximum atom-cavity coupling constant and the decay rates of the atomic polarization and the cavity field are  $(g_0, \gamma, \kappa)/2\pi = (16, 3, 1.4)\text{ MHz}$ , respectively.

A sample trace of a trapping event is presented in Fig. 3. Shown is the cavity transmission of the near-resonant probe laser at 780.2 nm and of the blue-detuned dipole laser providing the radial confinement. The persistent *axial* confinement at 772 nm (3 FSR detuned from the atom) ② amounts to a maximum potential height of  $U_a = h \times 346\text{ MHz}$ , with Planck constant  $h$ . The guiding field at 775 nm (2 FSR detuned from the atom) ③ produces a potential with height  $U_g = 2h \times 10.3\text{ MHz}$  [12]. The probe laser is on resonance with the bare cavity,  $\Delta_c = \omega_l - \omega_c = 0$ . Thus, the presence of an atom detunes the cavity from resonance and causes a decrease in the transmission. Slow atoms are guided to regions of strong coupling and cause sharp transmission drops ⑤. The trigger is armed  $t = 205\text{ ms}$  after launch of the atoms from the atomic fountain to select late atoms arriving with velocities below  $0.1\text{ m s}^{-1}$ . Upon detection of a strongly coupled atom in the cavity center (A), the atom is trapped by converting the transverse guiding mode to a confining doughnut mode ④ with a maximum potential height of  $h \times 30\text{ MHz}$ . Simultaneously, the probe intensity is reduced. When the atom leaves the mode, the cavity transmission increases to the bare cavity value for the reduced observation power (B). After each trapping event, the stabilization of all lasers and the cavity is checked ⑥.

Spectroscopy of the combined atom-cavity system allows us to determine the main characteristics of the blue trap. The experimental protocol consists of a sequence of alternating 0.5 ms long cooling and 0.1 ms short probing intervals. The probe detuning in the probe intervals is scanned with respect to the bare cavity frequency, which is 35(1) MHz blue detuned from the atomic frequency. During the cooling intervals the probe is on resonance with the bare cavity ( $\Delta_c = 0$ ) which allows for cavity cooling in the axial direction as well as independent qualification of the atom-cavity coupling [5]. A probe interval is qualified for having a strong atom-cavity coupling when the cavity transmission in the neighboring cooling intervals is below 10 % of the bare cavity transmission. The expectation value of the photon number in the cavity mode is calculated from the measured photon-detection rate and the known detection efficiency including propagation losses from the cavity to the detectors. Experimental results are displayed in Fig. 4. We purposely chose a large atom-cavity detuning,  $\Delta_c > 2g_0$ , with  $g_0/2\pi = 16\text{ MHz}$  the maximum atom-cavity coupling constant, to show that the blue trap preserves this detuning and allows to enter the regime of dispersive detection, as discussed below. Analytical results for an atom with fixed coupling (solid curve) fit the data (points) well. Comparison between theory and experiment gives an atom-cavity coupling constant of 83(12) % of  $g_0$ , much larger than the atomic and cavity decay rates. This proves that a strongly-coupled atom-cavity system has been prepared.

In Fig. 4, the measured Lorentzian transmission peak

of the bare cavity at  $\Delta_c = 0$  MHz is shown for reference. The bare atom is at  $\Delta_{ac}/2\pi = -35(1)$  MHz, with the uncertainty due to some residual magnetic field. The bare detunings are the same as those of the normal-mode experiment performed previously in a red dipole trap [11]. The obvious difference in the normal-mode spectra lies in the fact that in a red trap the atomic resonance is shifted by approximately twice the ground-state trap depth, effectively bringing the atomic transition frequency close to resonance with the cavity at the trap center (see Fig. 2 in [11]). In contrast, the normal-mode spectrum of an atom stored in the blue-detuned trap does not show any shift of the atomic frequency, as expected for an atom trapped at the node of the blue field. Since the large atom-cavity detuning is preserved, the character of the normal modes emerging from the bare states remain largely “atom-like” and “cavity-like”. The strong asymmetry of the peak heights arises from the fact that the system is excited via the cavity and observed in transmission. Therefore, the atom-like resonance is much weaker than the cavity-like resonance. The plots on shaded background are a blow-up of the spec-

trum ( $\sim 130\times$ ) to present the atom-like peak located at approximately  $\Delta_c/2\pi = -40$  MHz. This peak is slightly broadened by the spatial distribution of the atoms in the mode. A residual Stark shift  $\Delta_s/2\pi = 0.7(1.3)$  MHz can be derived from the analytical fit [13]. This shift is much smaller than the axial and radial trap heights,  $U_a = h \times 265(6)$  MHz and  $U_r = h \times 30(1)$  MHz, respectively. The Stark shift due to the red-detuned stabilization laser at 785.2 nm is  $\Delta_{stab}/2\pi = 2.2(1)$  MHz. The shift of the atomic transition frequency due to the blue trap is therefore smaller than the atomic linewidth.

The preservation of the large atom-cavity detuning facilitates dispersive measurements [10, 14, 15] while the blue trap provides confinement. This is exemplified by the detection of an atom in the cavity via the induced shift of the cavity-like normal mode. Such a measurement scheme keeps the atomic excitation low. To estimate the average number of spontaneously scattered photons during a certain observation time interval, we consider probing the system on resonance with the bare cavity. In the presence of a strongly coupled atom, the cavity transmission of the probe is reduced by a factor of  $\sim 20$ . The transmission is a direct measure of the excitation of the mode corresponding to  $\langle a^+a \rangle$  photons. In the limit of weak excitation the excitation probability of the atom is proportional to the photon number times the atomic Lorentzian:  $\langle \sigma^+\sigma^- \rangle = \langle a^+a \rangle g^2 / (\Delta_{ac}^2 + \gamma^2)$  where  $a^+(a)$  is the creation (annihilation) operator for

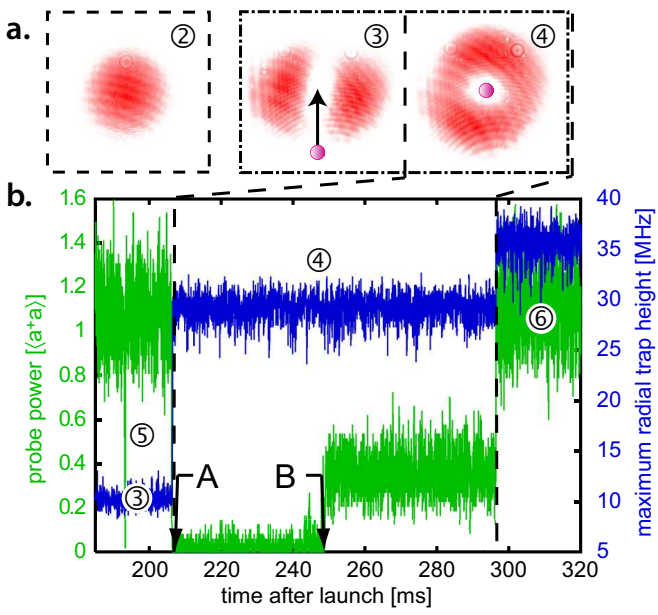


FIG. 3: (Color online) A blue-trapping event. a). Experimental intensity patterns of the different modes (cp. Fig. 1). b). Sample trace: Transmitted probe power in units of intra-cavity photon number,  $\langle a^+a \rangle$ , and the maximum radial trap height. Upon detection of an atom (A) the probe intensity is decreased and the trap is closed. When the atom leaves (B), the empty cavity transmission is observed. Experimentally, the “doughnut” mode ④ is a controlled superposition of two non-degenerate eigenmodes defined by our cavity. The trace is taken for detunings of continuous axial cavity cooling  $(\Delta_{ac}, \Delta_c)/(2\pi) = (-35, 0)$  MHz, where the average storage time for single trapped atoms is about 30 ms.

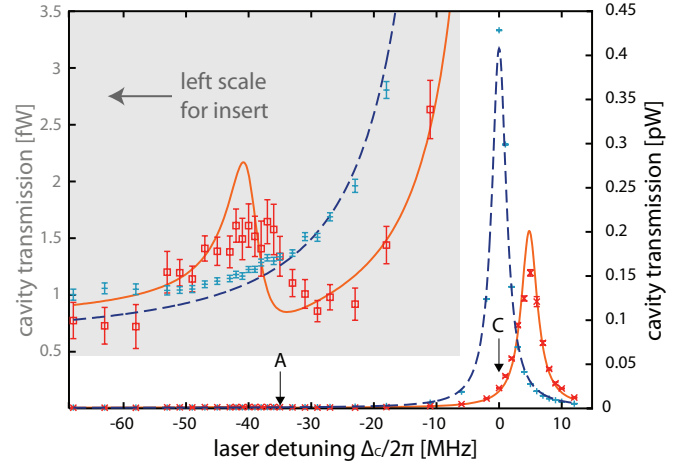


FIG. 4: (Color online) Normal-mode spectrum: transmission as a function of detuning for a well-coupled system (red squares and crosses). The bare atom (A) is detuned from the bare cavity resonance (C) by  $\Delta_{ac}/2\pi = -35$  MHz. A transmission of 1 pW corresponds to 1.2 intra-cavity photons. Intervals contribute to the spectrum if the transmission in the neighboring cooling intervals is  $< 10\%$  of the bare cavity value  $\langle n_0 \rangle$ . An analytical fit (solid line) for a fixed coupling  $g$  at low excitation results in  $g = 0.83(12) \times g_0$  and a residual Stark shift of  $\Delta_s/2\pi = 0.7(1.3)$  MHz. The empty cavity transmission (blue pluses, dashed line) is shown for reference.

cavity photons, and  $\sigma^+(\sigma^-)$  is the atomic raising (lowering) operator. The atomic excitation  $\langle\sigma^+\sigma^-\rangle$  is therefore given by the cavity excitation  $\langle a^+a \rangle = 0.022$  (cp. (C) in Fig. 4) times a constant which depends on the effective coupling,  $g$ , the atom-cavity detuning,  $\Delta_{ac}$ , and the atomic linewidth,  $\gamma$ . The effective coupling was deduced from the experimental data in Fig. 4, and  $\gamma$  and  $\Delta_{ac}$  are well known. The deduced average atomic excitation of  $\langle\sigma^+\sigma^-\rangle = 3.1 \times 10^{-3}$  leads to a scattering rate into free space given by  $2\gamma\langle\sigma^+\sigma^-\rangle \approx 117$  kHz. Thus, during a time interval of  $10\mu s$  the atom scatters 1.2(3) photons. This includes an overall experimental detection efficiency of 5% for photons lost from the cavity mode. A detailed analysis which assumes a 50% a priori probability of the presence of the atom in the cavity, i.e. maximum possible ignorance, and which takes into account the Poissonian statistics of the detected photons and all experimental imperfections, results in a 95% correct decision concerning the presence of the atom in this  $10\mu s$  long time interval. The required observation time interval scales inversely with the photon-detection efficiency which can be improved considerably.

While trapped, the atom heats up due to spontaneous emission and dipole-force fluctuations [8, 9]. The latter heating process is largely compensated by cavity cooling [5]. For the parameters of Fig. 3, the average storage time is about 30 ms. For a different trap height we also measured the storage time without the probe light to be about 20 ms. Moreover, we see the same dependence on the probe power as reported in Ref. [5], namely a trapping time decreasing inversely with increasing probe power. The observed trapping times are comparable to those found in a red trap [11] mainly because radial heating is not compensated for. An increase of the storage time by several orders of magnitude can be achieved for cavity cooling in three dimensions, which requires illuminating the system from the side [16]. In this scheme all probe lasers would be red detuned from both normal modes, such that light scattering increases the photon energy and, hence, cools the atom. Since in cavity cooling photons should predominantly be emitted via the cavity mode, this requires the lower dressed state to be “cavity-like”. An advantage of this cooling scheme would be that it is efficient for a strongly coupled atom at the trap center. Note that for a cooling laser resonant with the bare cavity ( $\Delta_c = 0$ ), as is the case in the experiment underlying Fig. 4, cooling is achieved only for an atom close to a node. As a first step in this direction, we have successfully captured and stored single atoms in the blue trap for the appropriate parameters for 3D cavity cooling.

In conclusion, we have realized a blue intracavity dipole trap which now allows measurements in cavity

QED while largely preserving the free-space level structure of the confined atom. Well controlled detunings and coupling are important for the investigation of genuine quantum effects, where a reliable coherent evolution is essential. For applications in quantum information science, the absence of differential energy shifts reduces dephasing of superposition states. Further perspectives for the blue trap include the possibility to control the atomic motion by means of feedback [17]. Such experiments would benefit from the possibility to independently address the radial and axial confinement. Moreover, in experiments where optical cavities are investigated as single-atom detectors [18, 19, 20, 21, 22] the blue “funnels” demonstrated in this Letter could efficiently guide atoms to regions of large atom-cavity coupling, thereby enhancing the detection efficiency.

---

\* Electronic address: gerhard.remppe@mpq.mpg.de

- [1] C. Monroe, *Nature* **416**, 238 (2002).
- [2] R. Grimm, M. Weidemuller, and Y. B. Ovchinnikov, *Adv. At. Mol. Opt. Phys.* **42**, 95 (2000).
- [3] J. Ye, D. W. Vernooy, and H. J. Kimble, *Phys. Rev. Lett.* **83**, 4987 (1999).
- [4] J. A. Sauer et al., *Phys. Rev. A* **69**, 051804(R) (2004).
- [5] P. Maunz et al., *Nature* **428**, 50 (2004).
- [6] S. Nußmann et al., *Phys. Rev. Lett.* **95**, 173602 (2005).
- [7] J. McKeever et al., *Phys. Rev. Lett.* **90**, 133602 (2003).
- [8] G. Hechenblaikner, M. Gangl, P. Horak, and H. Ritsch, *Phys. Rev. A* **58**, 3030 (1998).
- [9] K. Murr et al., *Phys. Rev. A* **74**, 043412 (2006).
- [10] P. Münstermann, T. Fischer, P. W. H. Pinkse, and G. Rempe, *Opt. Comm.* **159**, 63 (1999).
- [11] P. Maunz et al., *Phys. Rev. Lett.* **94**, 033002 (2005).
- [12] The maximum radial trap height in Fig. 3 is given for the doughnut mode. Since it scales with the ratio of the maximum intensity to the integrated intensity, the trap height for the TEM<sub>01</sub> guiding mode is a factor 2 larger.
- [13] A conservative upper bound for the Stark shift of  $\Delta_s/2\pi < 4$  MHz can be extracted from fitting only the slopes of the atom-like peak.
- [14] R. Quadt, M. Collett, and D. Walls, *Phys. Rev. Lett.* **74**, 351 (1995).
- [15] C. J. Hood, M. S. Chapman, T. W. Lynn, and H. J. Kimble, *Phys. Rev. Lett.* **80**, 4157 (1998).
- [16] S. Nußmann et al., *Nature Phys.* **1**, 122 (2005).
- [17] T. Fischer et al., *Phys. Rev. Lett.* **88**, 163002 (2002).
- [18] P. Horak et al., *Phys. Rev. A* **67**, 043806 (2003).
- [19] M. Trupke et al., *Appl. Phys. Lett.* **87**, 211106 (2005).
- [20] A. Öttl, S. Ritter, M. Köhl, and T. Esslinger, *Phys. Rev. Lett.* **95**, 090404 (2005).
- [21] T. Steinmetz et al., *Appl. Phys. Lett.* **89**, 111110 (2006).
- [22] I. Teper, Y.-J. Lin, and V. Vuletić, *Phys. Rev. Lett.* **97**, 023002 (2006).